



Label-free classification of growth-arrested state of cells by quantitative phase microscopy in fixative-treated cells

Mazaya Najmina, Nicholaus Kevin Tanjaya, Satoshi Ishii & Koichiro Uto

To cite this article: Mazaya Najmina, Nicholaus Kevin Tanjaya, Satoshi Ishii & Koichiro Uto (2025) Label-free classification of growth-arrested state of cells by quantitative phase microscopy in fixative-treated cells, Science and Technology of Advanced Materials: Methods, 5:1, 2525061, DOI: [10.1080/27660400.2025.2525061](https://doi.org/10.1080/27660400.2025.2525061)

To link to this article: <https://doi.org/10.1080/27660400.2025.2525061>



© 2025 The Author(s). Published by National Institute for Materials Science in partnership with Taylor & Francis Group



[View supplementary material](#)



Published online: 18 Jul 2025.



[Submit your article to this journal](#)



Article views: 13



[View related articles](#)



[View Crossmark data](#)

Label-free classification of growth-arrested state of cells by quantitative phase microscopy in fixative-treated cells

Mazaya Najmina^{a,b}, Nicholas Kevin Tanjaya^{b,c}, Satoshi Ishii^{b,c} and Koichiro Uto^{a,d}

^aResearch Center of Functional Materials, National Institute for Materials Science (NIMS), Tsukuba, Japan; ^bSubprogram in Materials Science and Engineering Graduate School of Science and Technology, University of Tsukuba, Tsukuba, Japan; ^cResearch Center for Materials Nanoarchitectonics (MANA), National Institute for Materials Science (NIMS), Tsukuba, Japan; ^dResearch Center for Macromolecules and Biomaterials, National Institute for Materials Science (NIMS), Tsukuba, Japan

ABSTRACT

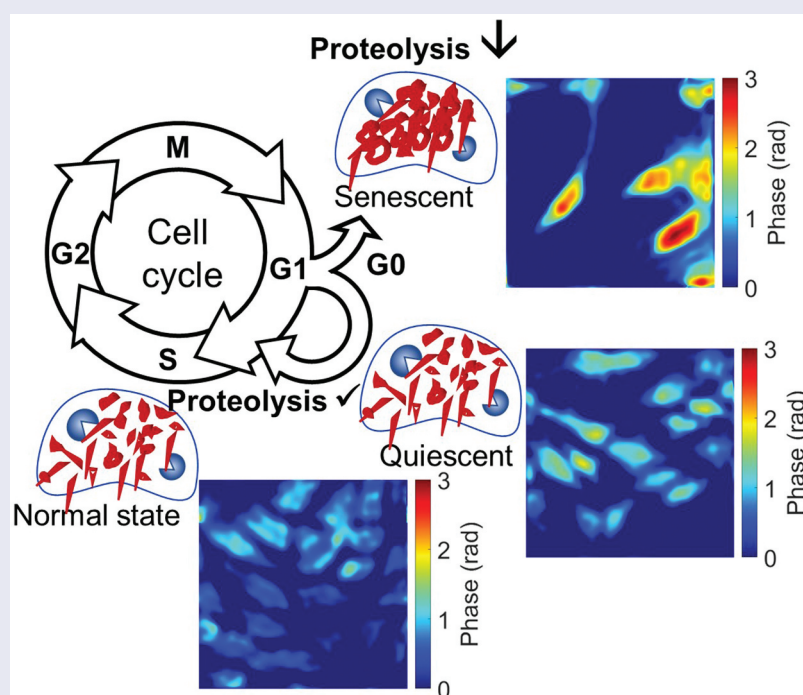
In the recurrence of cancer and autoimmune diseases, cellular senescence, a state where cells cease division, plays a pivotal role. Distinguishing the senescence requires a combination of multiple markers. Fluorescent dyes incorporation limits the imaging observation time due to the potential toxicity of those compounds over prolonged exposure, while colorimetric dye incorporation requires cell fixation, where cells are not in native state, and long staining time (≥ 4 hours). One of the distinct characteristics that distinguishes senescent cells from other state of cells is the impaired protein degradation ability by the lysosome, resulting on the protein accumulation. In the current work, we take advantage of protein accumulation to distinguish senescence cells from other cells. The protein concentration is visualized by recording the phase difference using the quantitative phase microscopy (QPM). Our live QPM observations on breast cancer cells confirm that senescent cells exhibit a higher refractive index compared to cells in normal growth and quiescent states, attributed to the accumulation of undigested lysosomal protein cargo. This heightened refractive index suggests an imbalance in protein turnover rates within senescent cells. These findings shed light on a potential label-free non-invasive approach for a prolonged monitoring of senescent cell dynamics.

ARTICLE HISTORY

Received 28 December 2024
Revised 16 June 2025
Accepted 17 June 2025

KEYWORDS

Growth arrest; label-free detection; senescence; quantitative phase microscope; protein concentration



IMPACT STATEMENT

We demonstrated the way to distinguish senescent cell from normal growth state visually by using quantitative phase microscopy based on the accumulation of undegraded intracellular protein.

CONTACT Satoshi Ishii  sishii@nims.go.jp  Research Center for Materials Nanoarchitectonics (MANA), National Institute for Materials Science (NIMS), 1-1 Namiki, Tsukuba, Ibaraki 305-0044, Japan; Koichiro Uto  UTO.Koichiro@nims.go.jp  Research Center for Macromolecules and Biomaterials, National Institute for Materials Science (NIMS), 1-1 Namiki, Tsukuba, Ibaraki 305-0044, Japan

 Supplemental data for this article can be accessed online at <https://doi.org/10.1080/27660400.2025.2525061>

© 2025 The Author(s). Published by National Institute for Materials Science in partnership with Taylor & Francis Group
This is an Open Access article distributed under the terms of the Creative Commons Attribution-NonCommercial License (<http://creativecommons.org/licenses/by-nc/4.0/>), which permits unrestricted non-commercial use, distribution, and reproduction in any medium, provided the original work is properly cited. The terms on which this article has been published allow the posting of the Accepted Manuscript in a repository by the author(s) or with their consent.

1. Introduction

The approval of cell cycle inhibitor as anticancer agent (Abemaciclib, Palbociclib) of hormone-receptor positive breast cancer by Food and Drug Administration (FDA) earlier this year and in the past few years implies the crucial role of cell growth regulation in directing tumor growth. Another disease, such as fibrosis, is driven by the ceased cell cycle arrest of renal cells at G2/M [1]. Growth arrest is a cellular state in which cells cease progressing through the cell cycle due to external stress, becoming arrested in a specific phase of the cell cycle. There are two types of growth arrest states in cells, depending on their ability to re-enter the cell cycle. Senescence represents a permanent growth arrest state, whereas quiescence is temporary. In a clinical context, it is essential to distinguish between cell states, including senescent, quiescent, and normal, in order to develop treatments that address all cell populations and avoid leaving behind any surviving cells. The growth arrested cell has been closely associated with breast cancer progression, where the presence of growth-arrested cell resulting from the low-dosage chemotherapy may contribute to the re-activation of cancer cells after adjuvant treatment. Recently, there has been significant development in senolytic drugs designed to selectively eliminate senescent cells within tumors. Real-time monitoring of senescence and distinguishing the senescent cell from quiescent cell and normal cell holds immense promise for the clinical application of senescent therapies, but it remains challenging [2]. The gold standard in detecting senescent cells is colorimetric staining using senescence-associated- β -galactosidase (SA- β -Gal) [3]. In addition to this, detecting senescent cells requires the combination of multiple markers and often involves fixing the cells or using fluorescent-based dye for live imaging. While fluorescent-based dyes, such as SPIDER- β -Gal, can be used for live-cell observation, they require the use of HEPES buffer during the dye incubation, which can impact cell morphology. This method may be less suitable for labelling epithelial cell types that rely on calcium to maintain cell-cell contact. Therefore, a label-free approach for classifying senescent cells presents an alternative solution to overcome these challenges.

To develop a label-free classification method, physical or chemical changes inside a cell associated with senescent cells should be identified. The senescent cell is generally known to have a slower protein synthesis rate and has been shown to amass extra protein residues as a consequence of impaired proteolytic capabilities and ceased cellular division [4]. Therefore, we hypothesized that the refractive index of senescent cells is elevated compared to that of normal or quiescent cells due to the accumulated undegraded

proteins. Changes in refractive index can be discerned by measuring optical phase difference. For this purpose, quantitative phase microscope (QPM) stands out as the most suitable technique.

Quantitative phase microscope literally measures optical phase quantitatively with the accuracy of milliradian or smaller. The optics of QPM is rather simple; it is based on a Mach-Zehnder interferometer, where quite often a commercial optical microscope is combined with a 4f optical system [5,6]. The Mach-Zehnder interferometer is widely used due to its well-established high sensitivity and resolution in quantitative phase imaging. A notable variation, diffraction phase microscopy (DPM), employs a common-path design to minimize phase noise from mechanical vibrations and air fluctuations, significantly improving measurement stability [5–7]. Thus far, QPM has been used to study cell cycle [7] and pathophysiology [8] of living cells

In the current work, we propose an approach to distinguish the growth-arrested state of cells from normal ones after fixative-treatment. In the experiments, the phase shifts of breast cancer cells were measured using our home-built QPM. The findings indicated a correlation between the total protein concentration in the breast cancer cell line and the observed phase difference obtained by QPM depending on the growth state of cells on fixative-treated cells.

2. Results and discussion

A subpopulation of breast cancer cells is known to undergo senescence post-treatment with clinical dosage of doxorubicin (DOX) within the range of hundreds of nanomolar [9]. The senescence of breast cancer cells is triggered by DOX treatment through the activation of p53 pathway [10]. In this study, epithelial (MCF-7) cell line was used as the model cell line instead of mesenchymal-like cell line (MDA-MB-231). This choice was based on MCF-7's lower sensitivity to DOX treatment compared to MDA-MB-231, attributed to its expression of estrogen receptor-alpha (ER α) [11]. Our result was consistent with those reports. Two days after treatment with a DOX concentration of less than 500 nM, the non-invasive MCF-7 breast cancer cells expressed early senescent markers, such as p53 and SA- β -Gal (Figure 1a and Fig. S1).

A 520-nm laser included in our QPM for imaging irradiated through three different cell states (normal, dormant, and senescent) inside a buffer and the transmitted phase images were reconstructed after the processing (Fig. S2 and Fig. S3). The recorded phase shift reflects the refractive index change of cells, which is supposed to depend on the protein concentration

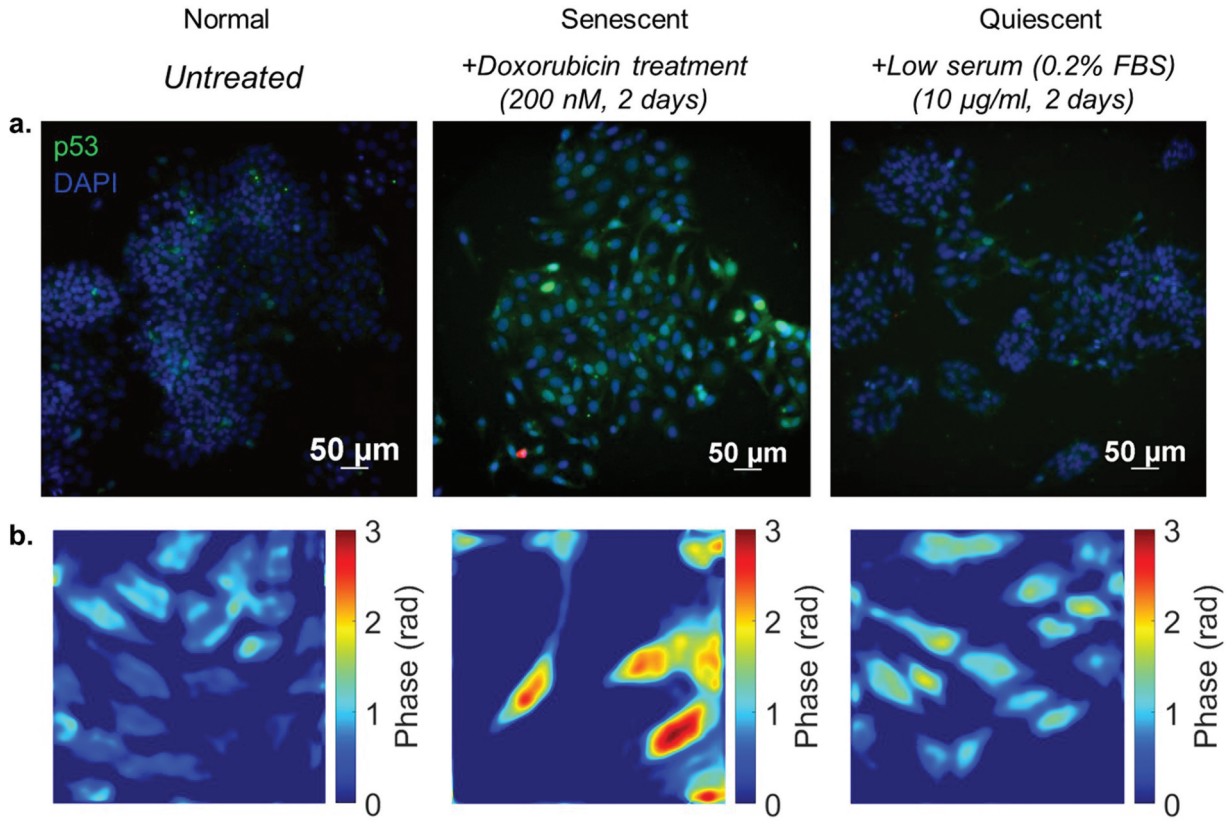


Figure 1. A. Expression of senescent marker protein, p53, detected by immunofluorescence for MCF-7 cells. b. Phase difference of MCF-7 cells observed by QPM after fixation of cells by using 4% paraformaldehyde (image size: 106.6 µm × 106.6 µm). Sub-figures a and b include images for normal, senescent, and quiescent states.

within the cells [12]. The inhibition of protein synthesis by Cycloheximide is reported to have negligible effect on the fatty acid synthase (FAS), enzyme that is responsible for saturated fatty acid production, expression in MCF-7 [13]. Since FAS was reported to remain relatively stable after cycloheximide treatment, it indicated that intracellular lipid production in MCF-7 is not inhibited. Therefore, we concluded that protein content is the main factor that induce the higher phase difference in induced senescent MCF-7. Therefore, the phase difference can be explained from Equation (1), where $\Delta\phi$, λ , n , C , and z are the phase difference, wavelength, refractive index, concentration, and axial distance from the surface, respectively.

$$\Delta\phi = \frac{2\pi}{\lambda} \int \Delta n(C) dz \quad (1)$$

The measured phase difference represents the state of the cells 2 days post treatment as exhibited in Figure 1b after subtracting with the background (phosphate buffer saline, PBS). From our observation, senescent breast cancer cells show around 2-fold higher phase difference than those in quiescent and normal states, as shown in Figure 1b. However, the phase difference between quiescent cells and cells in the normal growth state is not significant. The chosen cell seeding density resulted

in monolayer morphology with less than 80% confluency, thus the higher phase difference observed in senescent cell was not due to the overlapping cell growth. Doxorubicin treatment was reported to induce senescence also promoted actin polymerization in Huh7 cell line, which possesses epithelial-like morphology similar to MCF-7 cell line used in this study [14], leading to the enlarged cell morphology and cell flattening. Increased actin polymerization is correlated to the increased protrusion, thus leading to the cell flattening morphology (i.e. decreased thickness). In order to confirm the correlation between increased phase difference in senescent cells and impaired proteostasis, the cells in different growth states were treated with protein synthesis inhibitor, Cycloheximide (CHX). Following the inhibition of protein synthesis by CHX (Figure 2d), senescence-induced cells exhibit a 2-fold decrease in phase difference, reducing it to levels similar to those of normal cells (1–1.5). Considering that the cell thickness of MCF-7 may not change after senescent induction, these results both demonstrate that protein concentration in the cells is responsible for the observed phase difference among cells in different growth states, and impaired protein turnover is a key factor contributing to the high phase difference in the senescent cell.

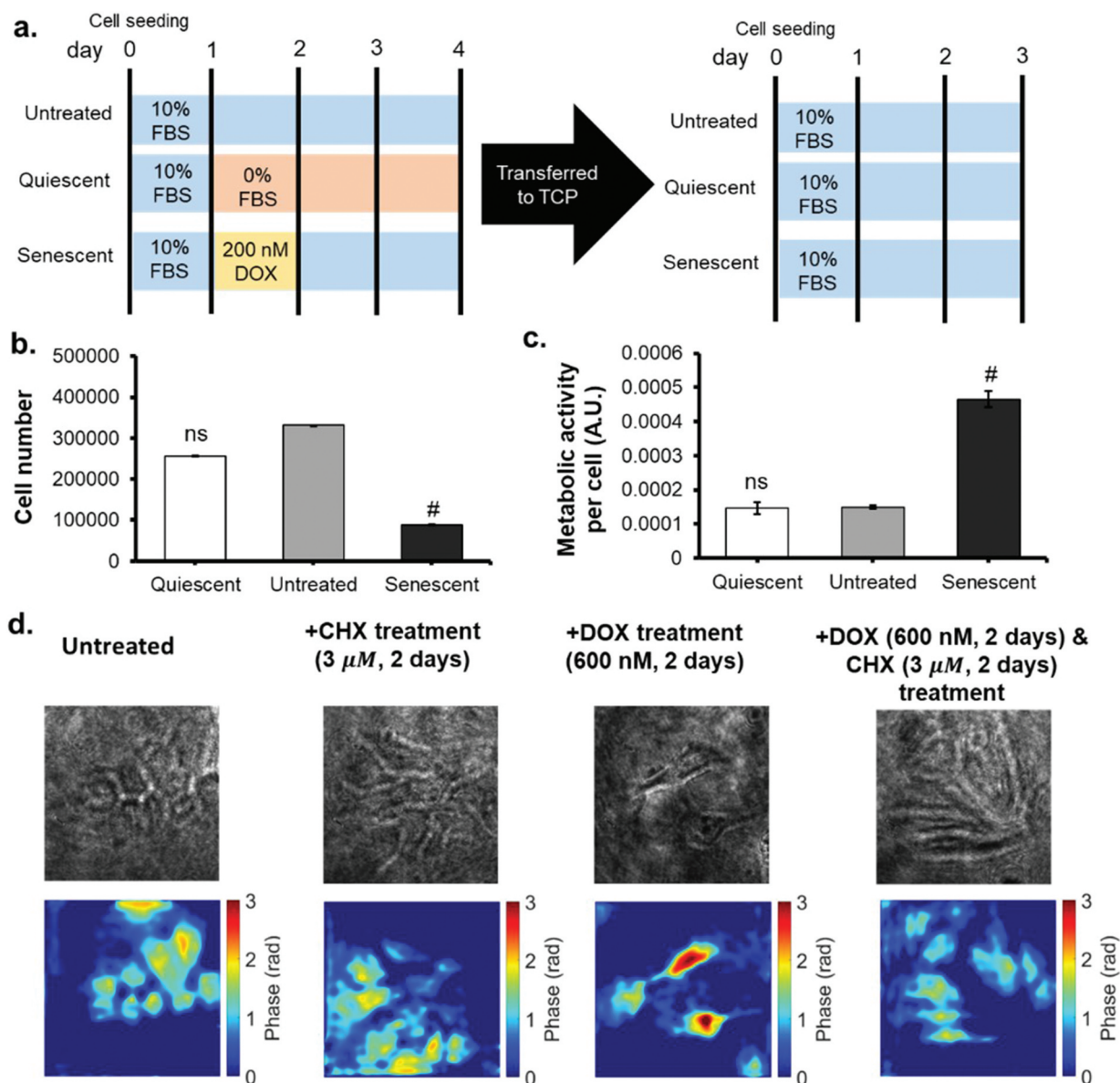


Figure 2. A. Schematic illustration of cell culture experiment to distinguish senescent cell from other states (cells were cultured on TCP dishes for 4 days and treated to induce different growth states, followed by transferring the cells into other TCP dishes supplemented with normal growth medium with 10% FBS). b. Proliferation behaviour comparison among different growth states of MCF-7 cells. Statistical study was performed by student’s t-test: # $p < 0.05$, not significant (n.S.) $p > 0.05$. All data are presented as mean \pm standard deviation ($n = 3$), c. Metabolic activity among different growth states of MCF-7 cells. Statistical study was performed by student’s t-test: # $p < 0.05$, not significant (n.S.) $p > 0.05$. All data are presented as mean \pm standard deviation ($n = 3$). d. Brightfield images (top) and phase images (bottom) of MCF-7 cell with different growth states, treated and/or non-treated with protein synthesis inhibitor drug, cycloheximide (CHX) taken after fixation of cells by using 4% paraformaldehyde (image size: 106.6 μ m \times 106.6 μ m).

The phase difference was observed due to the total protein concentration in the cells (Figure 3b). The senescent cells contain 1.5-fold higher protein concentration compared to the quiescent and normal cells, owing to their declined proteostasis [15]. A recent study reported the increasing protein concentration in lysosomes and mitochondria and a decrease in protein concentration in nuclei as cell size enlarged, which was observed in *in vitro* cultured senescent cells [16]. This higher total protein concentration in senescent breast cancer cells is consistent regardless of the

cellular compartment (nuclei or cytoplasm), as depicted in Figure 3(d,e). This is in line with the previously reported correlation between sub-compartmental protein concentration and cell size, in which, cytosolic protein concentration shows a small increase when the cell size enlarged [16]. The observed increase in cytosolic protein concentration in senescent cells is likely attributed to the accumulation of lysosomal cargo, a result of heightened cell metabolic activity (Figure 2(b,c)). It was previously reported that Adriamycin (doxorubicin)-induced

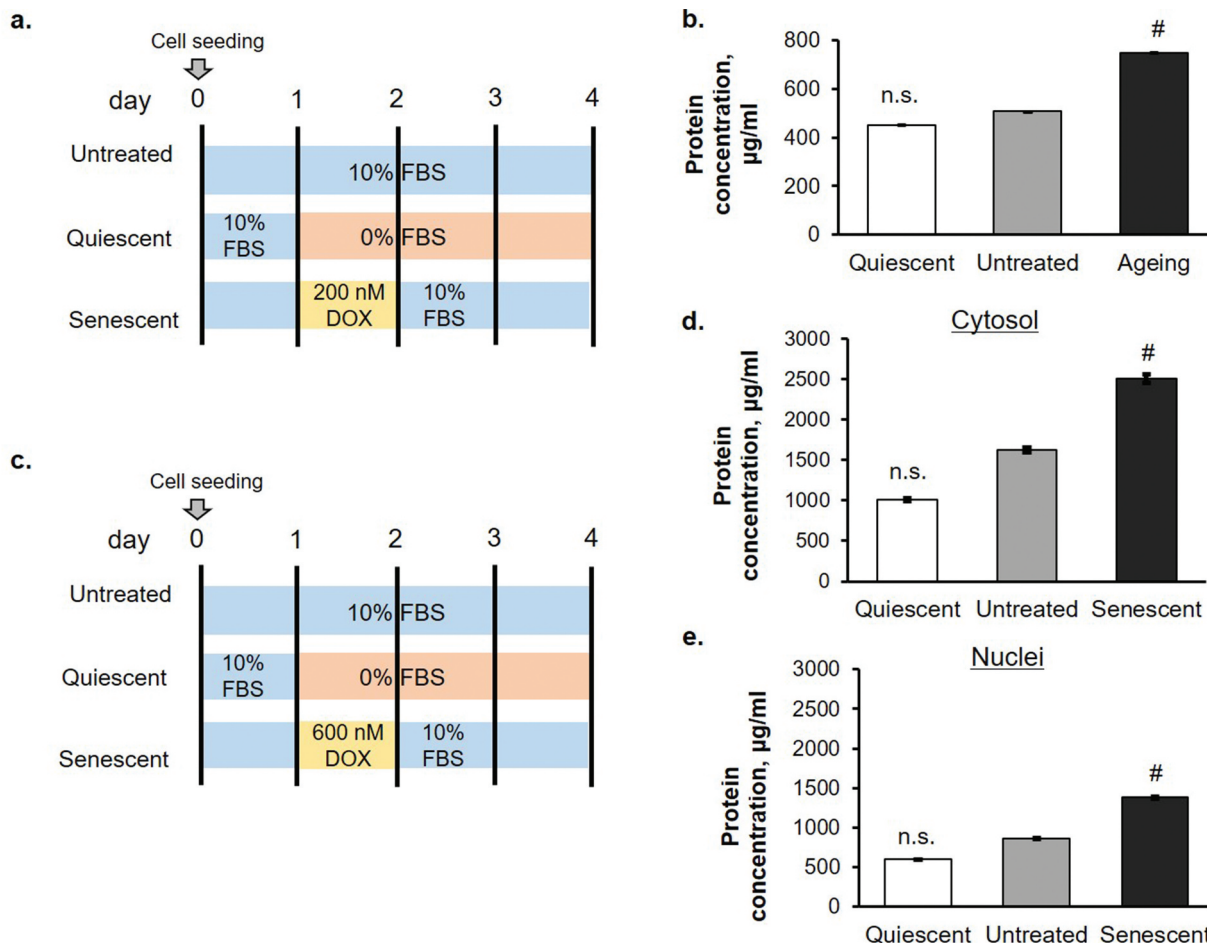


Figure 3. A. Scheme of cell culture experiment for evaluation of total protein concentration in cell (sub-panel b). b. Total intracellular protein concentration of MCF-7 cells determined by micro-BCA assay. Statistical study was performed by student’s t-test: # $p < 0.05$, not significant (n.S.) $p > 0.05$. All data are presented as mean \pm standard deviation ($n = 3$). c. Scheme of cell culture experiment for evaluating protein concentration in cytosol (sub-panel d) and nuclei (sub-panel e). d. Total cytosolic protein concentration of MCF-7 cells. Statistical study was performed by student’s t-test: # $p < 0.05$, not significant (n.S.) $p > 0.05$. All data are presented as mean \pm standard deviation ($n = 3$). e. Total nucleic protein concentration in MCF-7 cells with different growth states. Statistical study was performed by student’s t-test: # $p < 0.05$, not significant (n.S.) $p > 0.05$. All data are presented as mean \pm standard deviation ($n = 3$).

senescence of MCF-7 induced higher tricarboxylic acid (TCA) metabolism compared to untreated MCF-7 at day 5 after treatment [17].

The larger protein concentration in cytosol compared to the nuclei is observed in all samples, and it is not uncommon due to the presence of endoplasmic reticulum and golgi apparatus which contains proteins. The tendency of higher protein concentration in the nuclei in senescent cells compared to untreated cells is observed. This result may have been observed owing to the nuclear volume enlargement, a common trait of senescent cells [18]. The concentration of DOX for inducing a senescence state in MCF-7 cells has been adjusted to induce senescence in over 80% cell population. Thus, it is reasonable to assume that the metabolic activity of senescent cells was normalized across the entire senescence-induced cell population. This aligns with the known paradigm of senescence [19], in which senescent cells exhibit higher metabolic

activity than their untreated and quiescent counterparts and retain slower proliferation even after replating to the polystyrene dishes.

To further investigate whether the observed phase difference among different cell state is correlated with protein synthesis, live cell observation was performed. Protein synthesis primarily occurs during the cell cycle progression, specifically in G1 and G2 phases [20]. It is worth noting that mammalian cell division is known to occur over a 24 hour time course. While monitoring the dynamics of phase differences in cells during normal growth (Figure 4a, top), the cells exhibited an increase in phase difference until just before entering the division phase (M phase). Subsequently, a decrease in phase difference was noted in the resulting daughter cells following cell division (Fig S4c and d). In contrast, the dynamics of phase differences were not clearly observed in serum-starved cells that entered a quiescence state (Figure 4a, middle; Fig S4c and d).

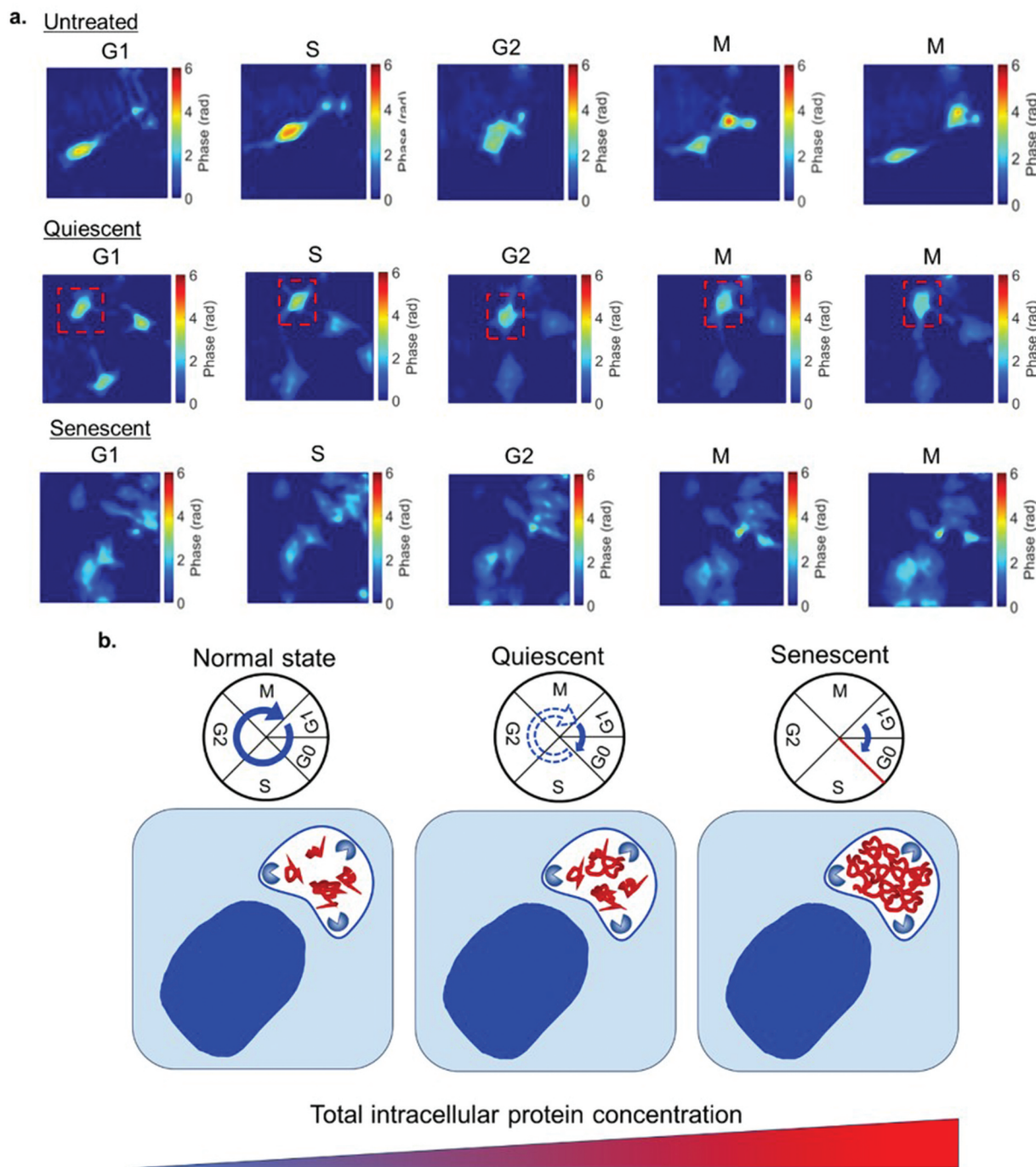


Figure 4. A. Timelapse image (image size: 106.6 mm × 106.6 mm) of living MCF-7 cells in normal growth state (top) vs quiescent (middle) vs senescent state (bottom) observed by QPM within 24 hours timeframe, showing the different phase change reflecting the difference of total intracellular protein amount during G1 and G2 stage of cell cycle (*G1 image is taken within 11 hours after the timelapse started, S image is taken within 5 hours post-G1 stage, G2 image is taken within 4 hours post-S stage, and M image is taken within 4 hours post-G2 stage). b. Proposed mechanism of observed phase difference driven by the growth state of MCF-7 cells.

Notably, senescence-induced cells exhibit an increase in phase difference until S phase, without experiencing decrease in phase difference, as they did not proceed to the division phase (Figure 4a, bottom; Fig S4c and d). However, there is a discrepancy between the phase shift obtained from fixative-treated cells and cells at the living state. We conducted a two-way ANOVA followed by Tukey’s HSD post hoc test. The analysis revealed significant effects of cell state in several cell cycle phases. In the G1

phase, cells in the untreated group showed significantly higher phase shift values compared to both quiescent ($p < 0.05$) and senescent ($p < 0.05$) groups (see Fig S4e; Table S1, S2). Therefore, our claim regarding the higher phase shift in senescent state compared to untreated and quiescent state is limited to the cells treated with fixative agent (Fig S4b). In the M1 phase, multiple pairwise differences between cell states were strongly significant with $p < 0.01$ (see Fig S4e). These results suggest that cell state

significantly influences phase shift-derived measurements, emphasizing intracellular process changes associated with cellular quiescence and senescence. The lower phase shift of senescent cells compared to the untreated cells at G1 stage suggests that larger number of representative cell population ($n > 3$) has to be employed in this characterization. This is because senescent-induced cells do not undergo cell division, resulting in a reduced cell population and consequently leading to an underestimated phase shift during the G1 phase. These findings demonstrate an alternative method in which QPM can effectively classify cell states based on the measured phase differences as an end-point assay. The results of QPM-based senescent cell detection were consistent with those obtained through staining-based and cellular functional assays. This study showed the positive correlation between QPM observation image and cellular functional assays of growth arrested cells (Fig S5), which also supports the previously reported studies [21,22]. In this study, we demonstrated the application of QPM in cellular imaging of cells at 2D system. The required transparent biological sample and a transmission microscope modality serve as major drawbacks of QPM, which pose to limit the potential of QPM for 3D biological systems. Moreover, the lack of chemical specificity of QPM remains an improvement point in the further study. The number of senescent cells is approximately less than 10% of cells throughout the body, yet it can influence the progression of many ageing related diseases. The experimental study in the senescence field commonly requires months or years to complete until the end-point assays. Therefore, non-invasive and real-time detection of senescent cells can allow continuous monitoring of growth arrest state progression without the need to sacrifice the cells. This protein synthesis events-based detection is not only limited to monitor the growth arrest state of cells. T cells energy production that is affected by protein synthesis regulates T cell-mediated immune response [23]. Thus, QPM is potentially a versatile approach for cell identification and functional evaluation based on cellular protein-synthesis ability [24].

3. Conclusion

This study shows the potential of QPM approach to observe the cellular fate change in breast cancer cell (MCF-7) visually when fixative treatment is used. In which, the phase change difference can be observed as the parameter to represent the change of cell growth state. We also demonstrated that the phase change difference observed by QPM positively correlate to the change of total intracellular protein amount that changed during the

progression of cell cycle. Based on this result, we propose a method to distinguish senescent cells from healthy cells visually after treated with fixative agent.

Acknowledgements

The authors would like to acknowledge Prof Mitsuhiro Ebara (NIMS and University of Tsukuba) for the fruitful discussion and support during the conduct of this work.

Disclosure statement

No potential conflict of interest was reported by the author(s).

Funding

This work was supported by JST FOREST Program, Grant Number [JPMJFR2327] (K.U.) and [JPMJFR2139] (S.I.), and a Grant-in-Aid for Transformative Research Areas (A) [JP20H05877] from the Japan Society for the Promotion of Science (JSPS KAKENHI).

Data availability statement

The data that support the findings of this study are openly available upon request.

References

- [1] Dimri GP, Lee X, Basile G, et al. A biomarker that identifies senescent human cells in culture and in aging skin in vivo. *Proc Natl Acad Sci.* 2020;92(20):9363–9367. doi: [10.1073/pnas.92.20.9363](https://doi.org/10.1073/pnas.92.20.9363)
- [2] Gil J. The challenge of identifying senescent cells. *Nat Cell Biol.* 2023;25(11):1554–1556. doi: [10.1038/s41556-023-01267-w](https://doi.org/10.1038/s41556-023-01267-w)
- [3] Liu X, Oh S, Peshkin L, et al. Computationally enhanced quantitative phase microscopy reveals autonomous oscillations in mammalian cell growth. *Proc Natl Acad Sci.* 2020;117(44):27388–27399. doi: [10.1073/pnas.2002152117](https://doi.org/10.1073/pnas.2002152117)
- [4] Frankowska N, Lisowska K, Witkowski JM. Proteolysis dysfunction in the process of aging and age-related diseases. *Front Aging.* 2022;3:927630. doi: [10.3389/fragi.2022.927630](https://doi.org/10.3389/fragi.2022.927630)
- [5] Bhaduri B, Edwards C, Pham H, et al. Diffraction phase microscopy: principles and applications in materials and life sciences. *Adv Opt Photon.* 2014;6(1):57–119. doi: [10.1364/AOP.6.000057](https://doi.org/10.1364/AOP.6.000057)
- [6] Tamamitsu M, Toda K, Shimada H, et al. Label-free biochemical quantitative phase imaging with mid-infrared photothermal effect. *Optica.* 2020;7(4):359–366. doi: [10.1364/OPTICA.390186](https://doi.org/10.1364/OPTICA.390186)
- [7] Tanjaya NK, Toda K, Ideguchi T, et al. Thermo-optical measurements using quantitative phase microscopy. *Opt Lett.* 2023;48(12):3311–3314. doi: [10.1364/OL.489182](https://doi.org/10.1364/OL.489182)
- [8] Sung Y, Tetrault MA, Takahashi K, et al. Dependence of fluorodeoxyglucose (FDG) uptake on cell cycle and dry mass: a single-cell study using a multi-modal

- radiography platform. *Sci Rep.* 2020;10(1):4280. doi: [10.1038/s41598-020-59515-0](https://doi.org/10.1038/s41598-020-59515-0)
- [9] Hou J, Yun Y, Xue J, et al. Doxorubicin-induced normal breast epithelial cellular aging and its related breast cancer growth through mitochondrial autophagy and oxidative stress mitigated by ginsenoside Rh2. *Phytother Res.* 2020;34(7):1659–1669. doi: [10.1002/ptr.6636](https://doi.org/10.1002/ptr.6636)
- [10] Jackson JG, Pant V, Li Q, et al. p53-mediated senescence impairs the apoptotic response to chemotherapy and clinical outcome in breast cancer. *Cancer Cell.* 2012;21(6):793–806. doi: [10.1016/j.ccr.2012.04.027](https://doi.org/10.1016/j.ccr.2012.04.027)
- [11] Wan X, Hou J, Liu S, et al. Estrogen receptor α mediates doxorubicin sensitivity in breast cancer cells by regulating E-cadherin. *Front Cell Dev Biol.* 2021;9:583572. doi: [10.3389/fcell.2021.583572](https://doi.org/10.3389/fcell.2021.583572)
- [12] Barer R. Refractometry and interferometry of living cells*†. *J Opt Soc Am.* 1957;47(6):545–556. doi: [10.1364/JOSA.47.000545](https://doi.org/10.1364/JOSA.47.000545)
- [13] Schroeder L, Kauffman A, Bigelow A, et al. Fatty acid synthase (FASN) regulates the mitochondrial priming of cancer cells. *Cell Death Dis.* 2021;12(11):102. doi: [10.1038/s41419-021-04262-x](https://doi.org/10.1038/s41419-021-04262-x)
- [14] Şimay YD, Ozdemir A, İbişoğlu B, et al. The connection between the cardiac glycoside-induced senescent cell morphology and Rho/Rho kinase pathway. *Cytoskelet Hob.* 2018;75(11):461–471. doi: [10.1002/cm.21502](https://doi.org/10.1002/cm.21502)
- [15] Sabath N, Levy-Adam F, Younis A, et al. Cellular proteostasis decline in human senescence. *Proc Natl Acad Sci.* 2020;117(50):31902–31913. doi: [10.1073/pnas.2018138117](https://doi.org/10.1073/pnas.2018138117)
- [16] Lanz MC, Zatulovskiy E, Swaffer MP, et al. Increasing cell size remodels the proteome and promotes senescence. *Mol Cell.* 2022;82(17):3255–3269.e8. doi: [10.1016/j.molcel.2022.07.017](https://doi.org/10.1016/j.molcel.2022.07.017)
- [17] You R, Dai J, Zhang P, et al. Dynamic metabolic response to adriamycin-induced senescence in breast cancer cells. *Metabolites.* 2018;8(4):95. doi: [10.3390/metabo8040095](https://doi.org/10.3390/metabo8040095)
- [18] Duran I, Pombo J, Sun B, et al. Detection of senescence using machine learning algorithms based on nuclear features. *Nat Commun.* 2024;15(1):1041. doi: [10.1038/s41467-024-45421-w](https://doi.org/10.1038/s41467-024-45421-w)
- [19] Lockhead S, Moskaleva A, Kamenz J, et al. The apparent requirement for protein synthesis during G2 phase is due to checkpoint activation. *Cell Rep.* 2020;32(2):107901. doi: [10.1016/j.celrep.2020.107901](https://doi.org/10.1016/j.celrep.2020.107901)
- [20] Alber AB, Suter DM. Dynamics of protein synthesis and degradation through the cell cycle. *Cell Cycle.* 2019;18(8):784–794. doi: [10.1080/15384101.2019.1598725](https://doi.org/10.1080/15384101.2019.1598725)
- [21] Aknoun S, Yonnet M, Djabari Z, et al. Quantitative phase microscopy for non-invasive live cell population monitoring. *Sci Rep.* 2021;11(1):4409. doi: [10.1038/s41598-021-83537-x](https://doi.org/10.1038/s41598-021-83537-x)
- [22] Bresci A, Kim JH, Ghislanzoni S, et al. Noninvasive morpho-molecular imaging reveals early therapy-induced senescence in human cancer cells. *Sci Adv.* 2023;9(37):eadg6231. doi: [10.1126/sciadv.adg6231](https://doi.org/10.1126/sciadv.adg6231)
- [23] Marchingo JM, Cantrell DA. Protein synthesis, degradation, and energy metabolism in T cell immunity. *Cell Mol Immunol.* 2022;19(3):303–315. doi: [10.1038/s41423-021-00792-8](https://doi.org/10.1038/s41423-021-00792-8)
- [24] Xin Z, Zhang C, Sun L, et al. High-performance imaging of cell-substrate contacts using refractive index quantification microscopy. *Biomed Opt Express.* 2020;11(12):7096–7108. doi: [10.1364/BOE.409764](https://doi.org/10.1364/BOE.409764)